# 5

# Narrowband Interference Suppression in Underwater Acoustic OFDM System

Weijie Shen, Haixin Sun*,
En Cheng, Wei Su and Yonghuai Zhang
*The Key Laboratory of Underwater Acoustic Communication and Marine Information Technology, Xiamen University, Xiamen, Fujian, China*

## 1. Introduction

In 1960, Chang [1] postulated the principle of transmitting messages simultaneously through a linear band-limited channel without ICI and ISI. Shortly after, Saltzberg [2] analyzed the performance of such a system and concluded, "The efficient parallel system needs to concentrate more on reducing cross talk between the adjacent channels rather than perfecting the individual channel itself because imperfection due to cross talk tends to dominate." This was an important observation and was proved in later years in the case of baseband digital signal processing.

The major contribution to the OFDM technique came to fruition when Weinstein and Ebert [3] demonstrated the use of the Discrete Fourier Transform (DFT) to perform the base-band modulation and demodulation. The use of the DFT immensely increased the efficiency of the modulation and demodulation processing. The use of the guard space and the raised-cosine filtering solve the problems of ISI to a great extent. Although the system envisioned as such did not attain the perfect orthogonality between sub-carriers in a time-dispersive channel, nonetheless it was still a major contribution to the evolution of OFDM systems.

In quest of solving the problem of orthogonality over the dispersive channel, Peled and Ruiz [4] introduced the notion of cyclic prefix (CP). They suggested filling the guard space with the cyclic extension of the OFDM symbol, which acts as if it is performing the cyclic convolution by the channel as long as the channel impulse response is shorter than the length of the CP, thus preserving the orthogonality of sub-carriers. Although addition of the CP causes a reduction of the data rate, this deficiency was more than compensated by the ease of receiver implementation.

Orthogonal Frequency Division Multiplexing (OFDM) scheme enables channel equalization in the frequency domain, thus eliminating the need for potentially complex time-domain equalization of a single-carrier system [5]. For this reason, OFDM has found application in a number of systems. Underwater acoustic(UWAC) OFDM system has been widely studied to overcome the complexity of underwater acoustic channels [6] and get a high speed data

* Corresponding Author

transmission. Nevertheless, due to the effect of"spectral leakage"in discrete Fourier transform(DFT)[7],which is used in OFDM receivers, spectrum of narrowband interference(NBI) will be spread in the whole frequency domain , thus, strongly impacts adjacent sub-channels [8-9].Various algorithms have been proposed for NBI suppression. Aiming at NBI suppression in OFDM systems, some approaches are employed. Receiver window method is well known as a simple and valuable NBI suppression technique [10]. Literatures [11] consider spreading the OFDM symbols over subcarriers using orthogonal codes. A linear minimum mean square estimator (LMMSE) for the NBI cancelation in frequency domain is introduced in [12]. Prediction error filter is introduced for mitigating the interference in the time domain, thereby preventing the spectralleakage of the interference power [13]. PEF is based on the fact that the OFDM signal can't be predicted since it has a flat spectrum, while the NBI can be predicted precisely. The effect of guard band in the PEF based NBI suppression is discussed, and two methods to solve this problem are discussed. It is shown that the proposed decimated prediction filter (DPF) and virtual subcarriers complement prediction error filter (VSC-PEF) outperform conventional PEF in OFDM systems with guard band [14]. Shi et. al [15] gave a comprehensive analysis of the impact of NBI on an OFDM based ultrawide- band (UWB) transceivers including ADC, timing and frequency synchronization. However, none has been done to examine how the NBI affects the cross-correlation based timing synchronization scheme [16], which has also been widely adopted. This paper examines this problem and provides theoretical analysis of timing synchronization of an OFDM system in the presence of multi-tone NBI. Numerical simulations are presented to verify the theoretical analysis. A Nyquist window is proposed for OFDM receiver without additional expense of system bandwidth, and choose the rectangular window and the raised cosine window window for analysis and simulation.The study was based on the experimental results in real underwater acoustic channel.[17]

This chapter is divided into five sections. Section 1.2 discusses the basic OFDM concept. The OFDM model is introduced in Section 1.3. Different kinds of window were described in Section 1.4, as well as Narrowband Interference Suppression methods in underwater acoustic communication systems. Simulation and experiment results were given in Section 1.5.

## 2. OFDM concept and its model

### 2.1 Evolution of OFDM

Frequency Division Multiplexing (FDM) has been used for a long time to carry more than one signal over a telephone line. FDM divides the channel bandwidth into sub-channels and transmits multiple relatively low rate signals by carrying each signal on a separate carrier frequency. To ensure that the signal of one sub-channel did not overlap with the signal from an adjacent one, some guard-band was left between the different sub-channels. Obviously, this guard-band led to inefficiencies.

In order to solve the bandwidth efficiency problem, orthogonal frequency division multiplexing was proposed, where the different carriers are orthogonal to each other. With OFDM, it is possible to have overlapping sub-channels in the frequency domain, thus increasing the transmission rate. The basis functions are represented in Figure 1. This carrier spacing provides optimal spectral efficiency.

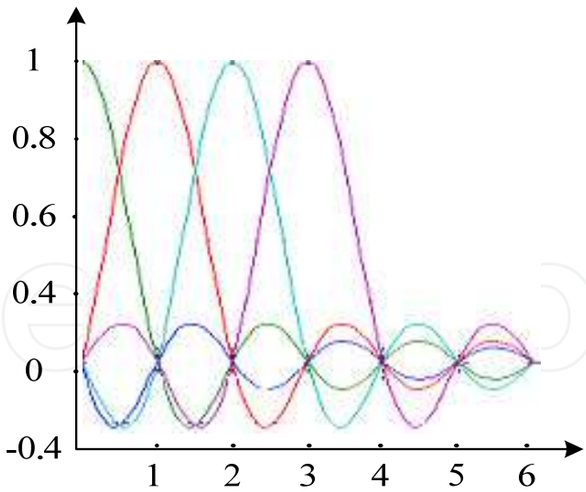


Fig. 1. Basis functions in OFDM system

Today, OFDM has grown to be the most popular communication system in high-speed communications.

### 2.2 Introduction to OFDM

The OFDM system studied in this paper has the block structure as shown in Figure 2. The system maps the input bits into complex-valued symbols $X(n)$ in the modulation block, which determines the constellation scheme of each sub-carrier. The number of bits assigned to each sub-carrier is based on the signal to noise ratio of each sub-carrier on the frequency range. The adaptive bit loading algorithm will be detailed below. The IFFT block modulates $X(n)$ onto N orthogonal sub-carriers. A cyclic prefix is then added to the multiplexed output of IFFT. The obtained signal is then converted to a time continuous analogy signal before it is transmitted through the channel. At the receiver side, an inverse operation is carried out and the information data is detected.

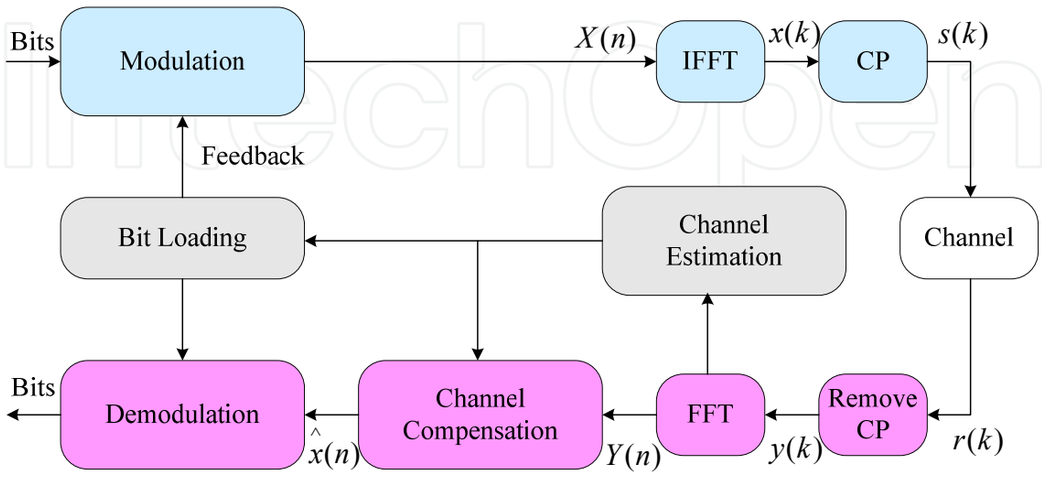


Fig. 2. OFDM system

### 2.3 FFT and IFFT

The key components of an OFDM system are the inverse FFT at the transmitter and FFT at the receiver. These operations performing linear mappings between N complex data symbols and N complex OFDM symbols, result in robustness against fading multi-path channel. The reason is to transform the high data rate stream into N low data rate streams, each experiencing a flat fading during the transmission. Suppose the data set to be transmitted is $X(1), X(2), ..., X(N)$, where N is the total number of sub-carriers. The discrete-time representation of the signal after IFFT is:

$$x(n) = \frac{1}{\sqrt{N}} \sum_{k=0}^{N-1} X(k) \bullet e^{-j2\pi k \frac{n}{N}}, \qquad n = 0 \ldots N-1 \tag{1}$$

At the receiver side, the data is recovered by performing FFT on the received signal,

$$Y(k) = \frac{1}{\sqrt{N}} \sum_{n=0}^{N-1} x(n) \bullet e^{-j2\pi k \frac{n}{N}}, \qquad k = 0 \ldots N-1 \tag{2}$$

An N-point FFT only requires $N \log(N)$ multiplications, which is much more computationally efficient than an equivalent system with equalizer in time domain.

### 2.4 Cyclic prefix

In an OFDM system, the channel has a finite impulse response. We note $t_{\max}$ the maximum delay of all reflected paths of the OFDM transmitted signal, see Figure 3.

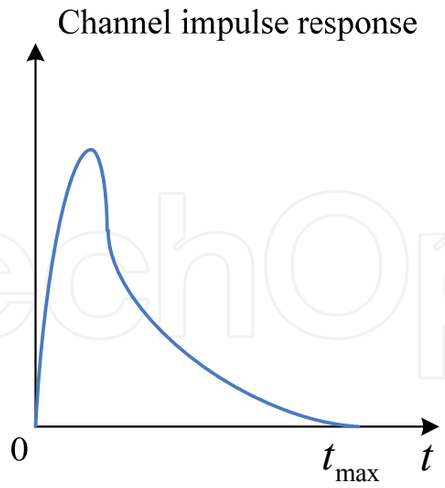


Fig. 3. Channel impulse response

Cyclic prefix is a crucial feature of OFDM to combat the effect of multi-path. Inter symbol interference (ISI) and inter channel interference (ICI) are avoided by introducing a guard interval at the front, which, specifically, is chosen to be a replica of the back of OFDM time domain waveform. Figure 4 illustrates the idea.

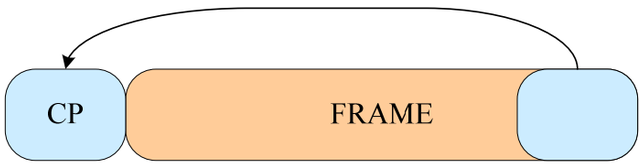


Fig. 4. Adding a cyclic prefix to a frame

From above expressions the sub-carrier waveforms are now given by

$$s(k)=\begin{cases} x(k+N) & -M\le k<0 \\ x(n)=\frac{1}{\sqrt{N}}\sum_{k=0}^{N-1}X(k)\bullet e^{j2\pi k\frac{n}{N}} & 0\le k<N-1 \end{cases} \tag{3}$$

The idea behind this is to convert the linear convolution (between signal and channel response) to a circular convolution. In this way, the FFT of circular convolved signals is equivalent to a multiplication in the frequency domain. However, in order to preserve the orthogonality property, $t_{\max}$ should not exceed the duration of the time guard interval. Once the above condition is satisfied , there is no ISI since the previous symbol will only have effect over samples within $[0,t_{\max}]$. And it is clear that orthogonality is maintained so that there is no ICI.

$$r(k)=s(k)\otimes h(k)+e(k) \tag{4}$$

$$\begin{aligned} Y(n)&=DFT(y(k))=DFT(IDFT(X(n))\otimes h(k)+e(k)) \\ &=X(n)\bullet DFT(h(k))+DFT(e(k)) \\ &=X(n)\bullet H(n)+E(n) \qquad ,0\le k\le N-1 \end{aligned} \tag{5}$$

where $\otimes$ denotes circular convolution and $E(n)=DFT(e(k))$. Another advantage with the cyclic prefix is that it serves as a guard between consecutive OFDM frames. This is similar to adding guard bits, which means that the problem with inter frame interference also will disappear.

### 2.5 Modulation and demodulation

Given the adaptive bit loading algorithm, the modulator has a number of bits and an energy value as input for each sub-carriers. The output for one sub-carrier is a constellation symbol with a desired energy, corresponding to the number of bits on the input. The modulator is taken to get either 2bits, 4bits, 6bits or 8bits available, which means that, respectively, only QPSK, 16QAM, 64QAM and 256QAM are available for modulation on each sub-carrier.

Demodulation is performed using Maximum Likelihood (ML) approach, given knowledge of the flat fading channel gain for each sub-carrier.

Furthermore, in order to reduce bit errors, Gray-coded constellations are also employed for each modulation order available. This Gray coding ensures that if a symbol error occurs, i.e. the decoder selects an adjacent symbol to what the transmitter intended to be decoded, there is only a single bit error resulting.

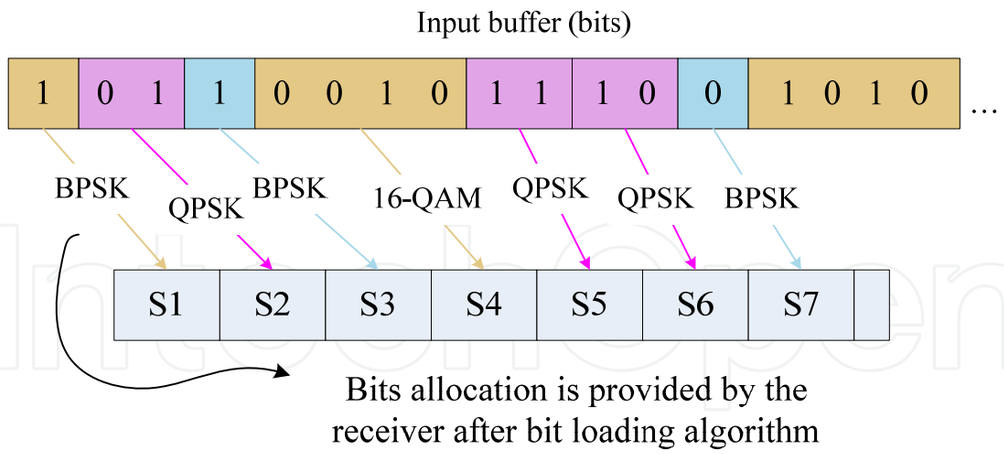


Fig. 5. Bits allocation in modulation

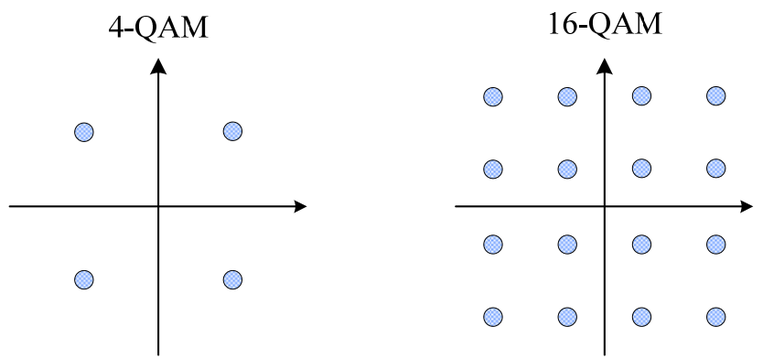


Fig. 6. 4-QAM(left) and 16-QAM(right)

Large performance improvement can be obtained in this adaptive modulation application where the modulator basis functions are designed as a function of measured channel characteristics. On good sub-channel (high SNR), modulation methods, such as 64 QAM, are used to increase the bit rate. And a lower modulation, such as QPSK, is performed on bad sub-channel to keep the error rate in a low level.

### 2.6 Interference

The interference signal selected is a non-orthogonal sinusoid relative to the OFDM waveform orthogonal basis set and has been added in the physical layer as part of the channel. A non-orthogonal interference signal has been selected because the zeros of the spectral response of the non-orthogonal interference signal do not fall on the zeros of the spectral response of the OFDM orthogonal basis set. As shown in figure 7, the difference in the spectral responses of the two types of interference signals measured at the zero crossings of the orthogonal basis set of the OFDM wave-form vary by 350 dB, which is limited by the computational precision of the algorithm. The result is the spectral side-lobes of the non-orthogonal interference signal corrupt each channel of the OFDM waveform, whereas the orthogonal interference signal corrupts only one channel.

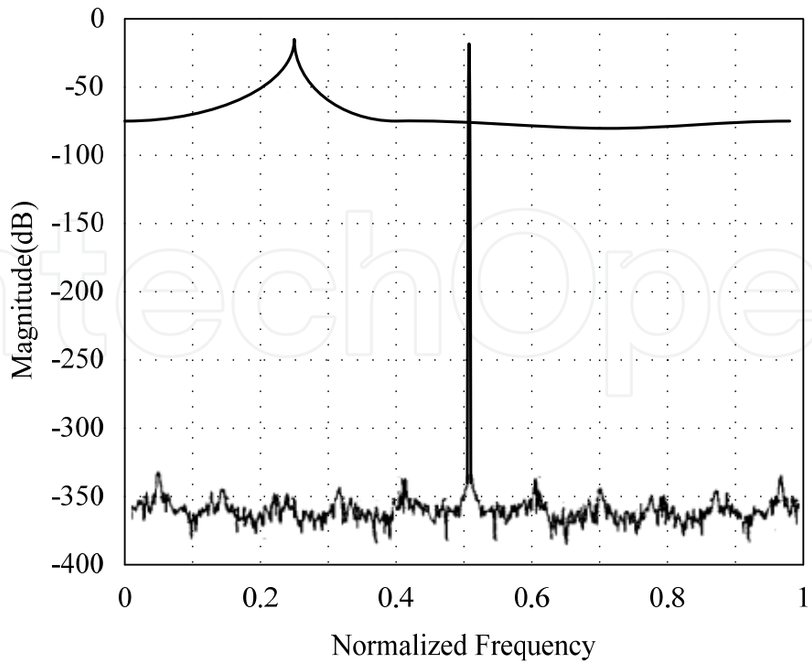


Fig. 7. Spectral Characteristics of the Interference Signal used to Demonstrate the Difference Between an Orthogonal and Non- Orthogonal Interference Signal

Figure 8 summarizes the simulation results for measuring the bit error rate vs. $E_b / N_0$ in the presence of the non- orthogonal interference signal. The reference BER vs. $E_b / N_0$ curve has no interference signal added in the physical layer. The interference signal amplitude was varied relative to the energy in one channel in the OFDM waveform to measure the degradation in performance. For a OFDM modulator implemented as a $2N$ point DFT, the energy in either the in-phase or the quadrature component of one channel is given by the expression:

$$E_S = \frac{1}{2N}\overline{a^2} \tag{6}$$

where $\overline{a^2}$ is the average one-dimensional constellation energy of the input source and N is the number of channels per OFDM waveform. It should be noted that practical OFDM waveforms usually have a minimum of 2048 channels to extend the OFDM waveform duration for protection against fading. For high values of $E_b / N_0$, simulations require a large number of Monte Carlo iterations in order to have results that are statistically significant. For this simulation 500 Monte Carlo iterations have been selected. For $N$ equal to 32 and the average one-dimensional constellation energy of the input source equal to 0.43 for 64-symbol QAM, the average energy per channel is:

$$\overline{\mathrm{E}_s} = \frac{0.43}{2(32)} = 6.7(10)^{-3} \tag{7}$$

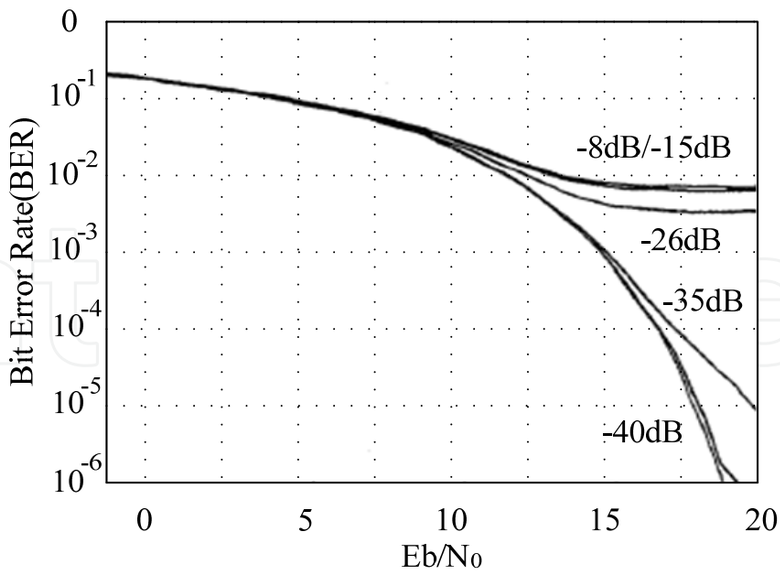


Fig. 8. Bit Error Rate vs. $E_b / N_0$ for Uncompensated OFDM with Varying Signal Energy from-8 dB to-40dB Relative to the Energy in one Channel.

As shown in figure 8, degradation in bit error rate is seen for interference signals that have signal energies larger than 40 dB below the energy in one channel of the OFDM wave-form. For interference signals with larger amplitude levels, the performance degradation quickly approaches a bit error rate of approximately $(10)^{-2}$ independent of $E_b / N_0$ .

## 3. Narrowband interference suppression

### 3.1 Narrowband interference analysis

Narrow-band Interference are Single-frequency sinusoidal signals [18], which can be approximated as follows:

$$i(t) = a \cdot e^{(j2\pi f_c t + \theta)} \tag{8}$$

Where $f_c$ is the interference frequency, and $\theta$ is a Random phase offset. Generally, the $k^{th}$ sample of the baseband received signal in time domain can be represented as

$$r(k) = \sum_{i=-\infty}^{+\infty} s(i) \cdot h(k-i) + n(k) + i(k) \tag{9}$$

where $s$ is a diagonal matrix containing the transmitted signalling points, $h$ is a channel attenuation vector, $n$ is a vector of independent identically distributed complex zero-mean Gaussian noise with variance $\sigma_n^2$ . The noise $n$ is assumed to be uncorrelated with the channel $h$ .And $i$ is the interference. After FFT we got

$$R_{k,n} = H_{k,n} S_{k,n} + N_{k,n} + I_{k,n} \tag{10}$$

$R_{k,n}, H_{k,n}, S_{k,n}, N_{k,n}$ and $I_{k,n}$ represent the corresponding $k^{th}$ frequency domain coefficient in the nth symbol. Where

$$I_{n,k} = \frac{\alpha \sin(\pi(\hat{f}N - K))}{N \sin(\pi(\hat{f} - K/N))} e^{j\pi(N+1)(\hat{f}-K/N)} \tag{11}$$

In the above equation, $\hat{f}$ is the normalize narrowband interference central frequency, $\hat{f} = f_c / f_s$, where $f_s$ is the sampling frequency of OFDM symbols.

### 3.2 Leakage of narrowband interference and its suppression methods

#### 3.2.1 The FFT filter bank

In the receiver, the analog OFDM signal passes the anti-alias filter before being sampled at a rate $f_a = 1/T_a$.We assume the baseband signal is a complex low-pass signal without oversampling, therefore we obtain $N$ complex samples each $T_u$ and $G$ samples each $T_g$.The $k^{th}$ sample $\underline{b}_k$ of a symbol is

$$\underline{b}_k = \sum_{i=1}^{N} \underline{c}_i e^{j2\pi f_i \cdot k \cdot T_a} \tag{12}$$

with $|f_i - f_{i-1}| = f_t$. The first step to recover carrier orthogonality is to eliminate for each symbol the $G$ samples of the guard interval, as shown in figure 9. After that a discrete

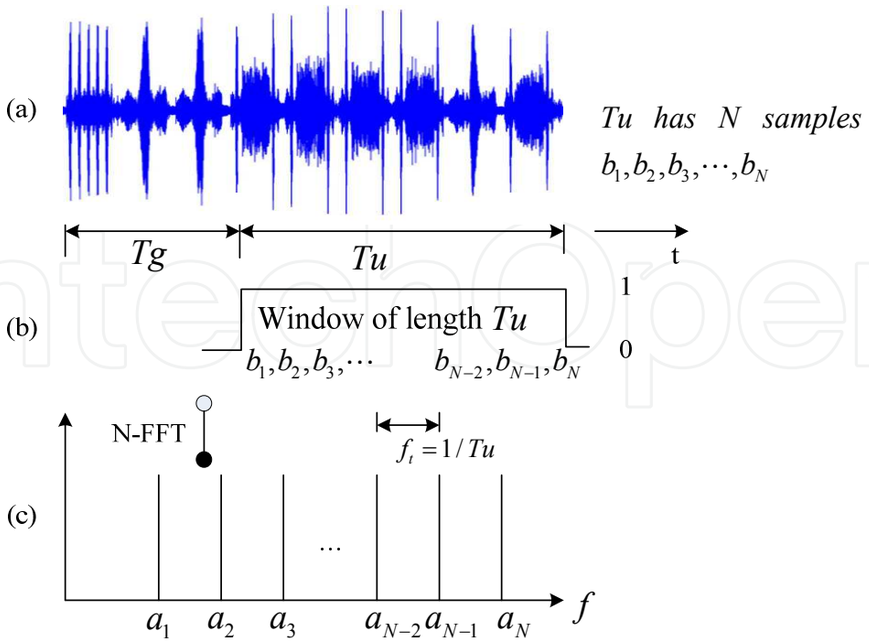


Fig. 9. a) OFDM-Symbol in time domain(top); b) selection of $T_u$ using a square window(middle); c) OFDM-symbol in frequency domain(below)

Fourier transform DFT of the remaining $N$ samples forces the periodicity of the time signal. The DFT performs the carrier filtering without inter-carrier-interference ICI, provided that $T_u = 1/f_t = NT_a$. The obtained complex coefficients $a_n$ contain the original amplitude and phase information of the $n^{th}$ respective carrier. The orthogonaly filtered $N$ carriers are shown in figure 9.

Using the proposal in [5] the filtering of each OFDM carrier is made with an FFT. The FFT has been considered in [19, 20] as a filter bank. The DFT $X(n)$ of a sampled signal $x(k)$ is defined

$$X(n) = \sum_{k=0}^{N-1} x(k) \bullet e^{-jkn\frac{2\pi}{N}} \tag{13}$$

Being $F$ the normalized discrete frequency, whereby $F = N \cdot f / f_a$, the frequency response of the $n^{th}$ filter $H_n(F)$ is

$$|H_n(F)| = \left| \frac{\sin[\pi(F-n)]}{\sin[\pi(F-n)/N]} \right| \tag{14}$$

which is shown in figure 10 for $n = 16$. Due to the properties of the DFT this frequency response is periodical, with $|H_n(F-n)| = |H_n(F-n+N)|$. The integration of power components covered by the frequency response in figure 10 leads to the amplitude of FFT coefficient $a_{16}$.

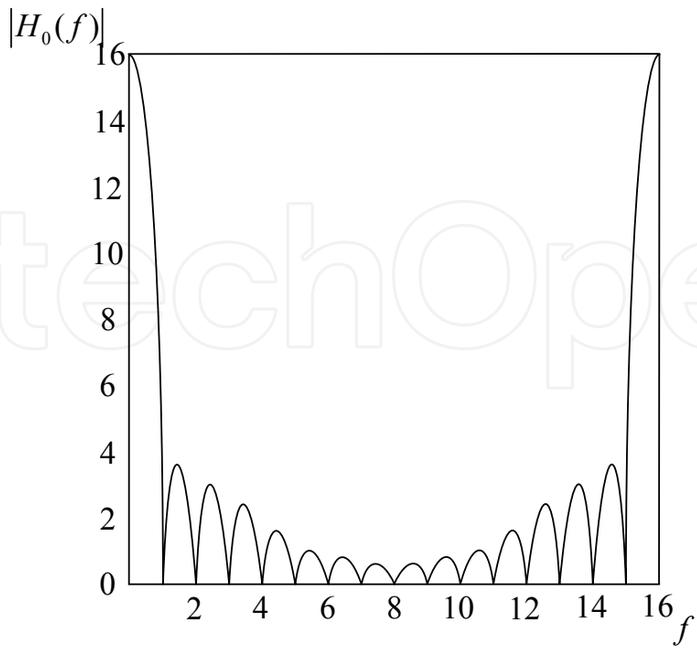


Fig. 10. Frequency response of a DFT filter ( $n = 16$ )

The reason why the DFT presents the frequency response in figure 10 is because the DFT performs the transform in blocks of only $N$ samples, as shown in figure 9. This is equivalent to using a square window in time domain of length $T_u$ corresponding to a $\sin(x)/x$ function in frequency domain. Due to the sampling in time domain, the frequency response is forced to periodicity leading to aliasing between the $si(x)$ functions. Therefore the (periodical) frequency response of the DFT is an aliased $si(x)$ function, also known as the Dirichlet function. Figure 11 shows the DFT filter bank consisting of $N$ filters having the same shape of figure 10 but different center frequencies.

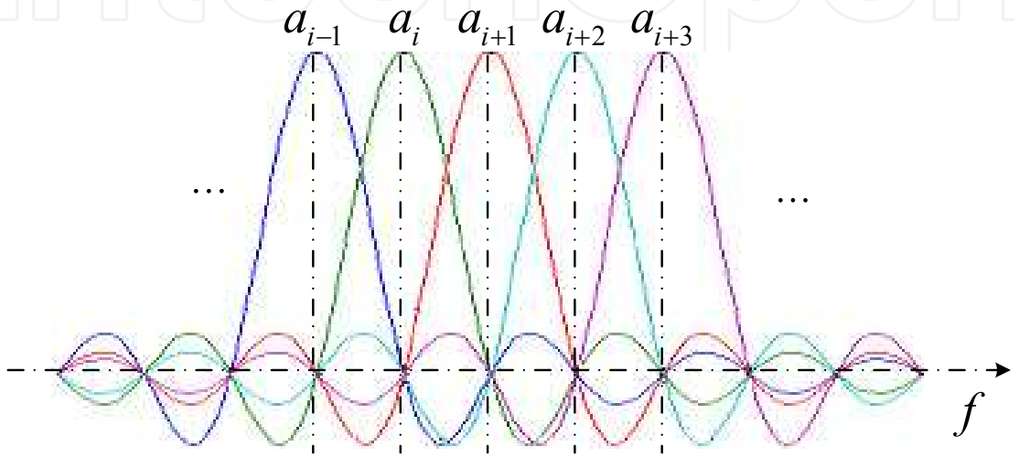


Fig. 11. Position of carriers in the DFT filter bank

The carriers are represented by ideal Dirac distributions placed on the filter maxima. The maximum of one filter coincides with the zero crossing of all others; this fact allows to separate the carriers without suffering any ICI. The interference occurs only for frequency components which does not correspond with the filter maxima.

In the non-ideal receiver the carriers are not exactly placed on the filter maxima due to frequency deviations producing the "leakage" of the DFT. This effect is explained in figure 12. The DFT of a single carrier without leakage *(F = 5)* consists of only one frequency component (FFT coefficient $a_5 = 16$), which includes the whole energy of the signal. In case of leakage *(F* = 4.7) the energy of the original carrier is distributed over all other frequency components (coefficients). The OFDM signal, consisting of many carriers which now "see" each other, is disturbed by IC1 due to leakage.

Leakage occurs also in case that the carriers are disturbed by phase noise leading to a widening of spectrum floor. White noise and disturbances like sine spurious also causes leakage. Nevertheless it is important to note that the leakage does not change the total signal power. The addition of the squared components (power) of figure 12 is always the same (256) independent of the carrier frequency [19, 20].

The DFT filter has the main disadvantage that its frequency response extends over the whole frequency range and presents high side lobes which decrease relatively slowly in frequency. Due to this fact the OFDM signal is very sensitive to frequency deviations and

phase noise and discrete spurious. Therefore we need a filter bank with improved frequency response which keeps orthogonality that is easy to implement. The last requirements may be fulfilled using a nyquist windowing before computing the FFT.

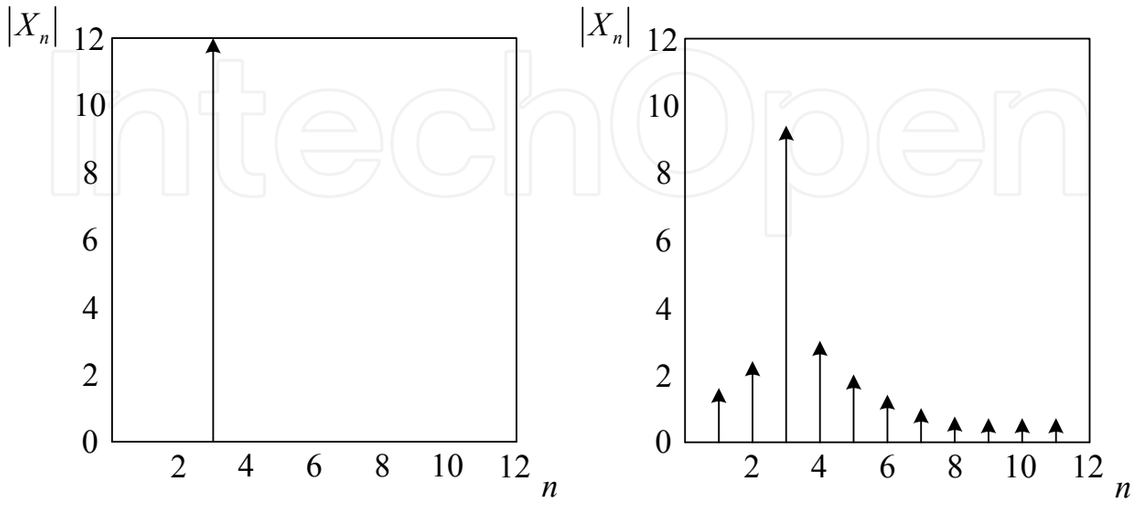


Fig. 12. DFT of a sine wave with leakage (left) and without leakage (right)

### 3.2.2 Using a Nyquist window in time domain

The use of a window e.g. Kaiser on the $N$ samples before the FFT reduces the side lobe amplitude but also leads to an orthogonality loss between carriers. A windowing which reduces the side lobes and conserves the carrier orthogonality is called Nyquist window. It needs a repetition of every symbol in order to be implemented. For this purpose, the guard interval will be used. Since in many cases only a piece of the guard interval is necessary in order to avoid ISI, the other "usable" part of the guard interval may be used for the Nyquist windowing. Nevertheless $2N$ samples are necessary in order to maintain the orthogonality, as shown next.

The adaptive Nyquist windowing is able to improve the frequency response of the DFT filter. This windowing may be implemented with a guard interval length between $0$ and $T_u$, $T_u \geq T_g \geq 0$. In case of a multi-path reception only the "usable guard interval" $T_v$ (variable length) is used for the windowing. $T_v$ is supposed to be free of ISI. The windowing is adaptive because $T_v$ depends on modulation parameters and channel conditions. Figure 13 shows the way to implement an adaptive Nyquist windowing, as used in [21].

The usable part of the guard interval $T_v$, $T_v$ consists of $V$ samples. The $V$ samples of $T_v$ together with the OFDM-symbol $T_u$ ($N$ samples) are symmetrically windowed. The window $w(t)$ has a shape which fulfills the time domain analogy to the Nyquist criterion. Defining the "Nyquist time" $T_u$ we expect to have no IC1 (in frequency domain!) if the window shape is symmetrical to $T_u$. In the same manner as for a pulse shaping filter, we may choose the Nyquist window using a raised cosine function, shown in figure 14.

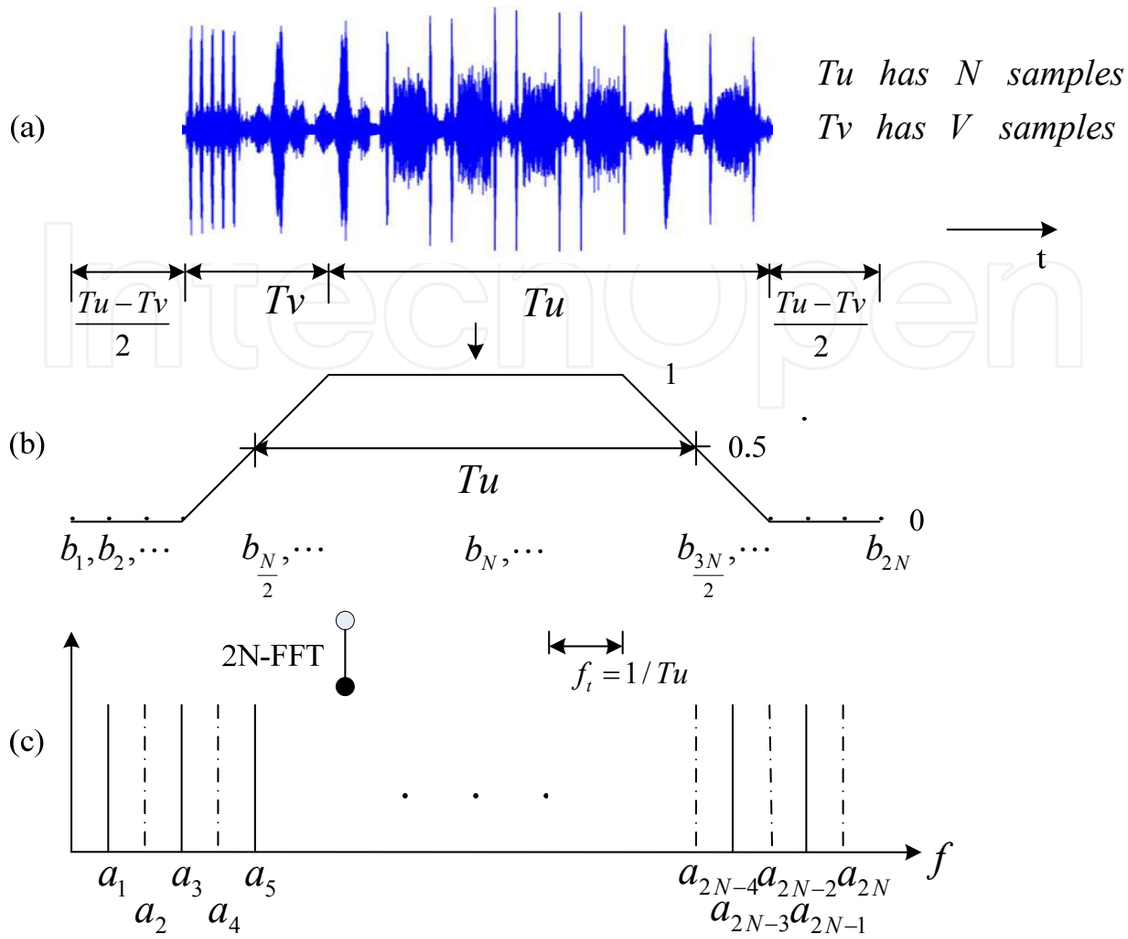


Fig. 13. OFDM-symbol using an adaptive Nyquist window a) In time domain, b) Nyquist window, c) Spectrum

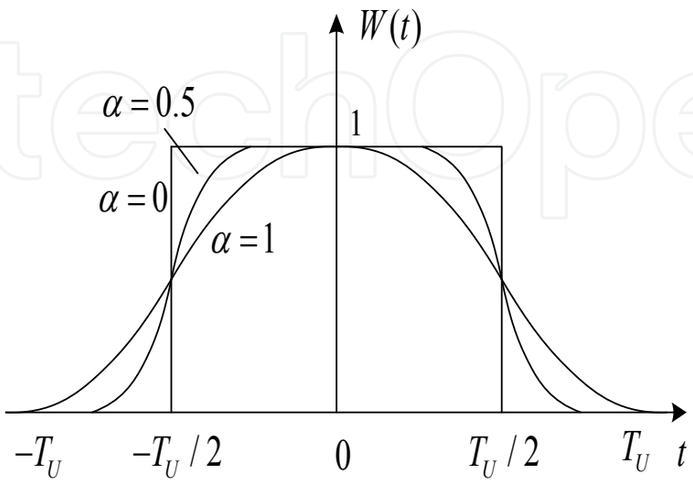


Fig. 14. Raised cosine window function w(t) depending of roll-off factor $\alpha$

$$w(t)=\begin{cases}1 & 0\le|t|\le\dfrac{(1-\alpha)T_u}{2}\\ \dfrac{1}{2}\left[1-\sin\dfrac{\pi(|t|-T_u/2)}{\alpha T_u}\right] & \dfrac{(1-\alpha)T_u}{2}\le|t|\le\dfrac{(1+\alpha)T_u}{2}\\ 0 & |t|\ge\dfrac{(1+\alpha)T_u}{2}\end{cases} \tag{15}$$

We define a roll-off factor $\alpha = T_v / T_u$, which varies depending on the usable part of the guard interval. Practical values of $\alpha$ between $0$ and $0.3$ may be considered.

After Nyquist windowing the filter bank has lost its orthogonality, since the zero crossings are separated by $1/(T_u+T_v)\neq f_{tr}$. Neither a FFT of the total windowed samples $V+N$ is possible, because their number is not a power of two. Thus a symmetrical "zero padding" is performed in order *to* complete a total of $2N$ samples $b_{k,w}$, where

$$b_{k,w}=\begin{cases}0 & 1\le k<(N-V)/2\\ b_k w(t) & (N-V)/2\le k\le 3(N+V)/2\\ 0 & 3(N+V)/2<k<2N\end{cases} \tag{16}$$

In this way a FFT may still be used instead of the more complex non-power-of-two-DFT and the filter bank orthogonality is restored. The FFT computes the $2N$ coefficients $\alpha_k$ on the windowed samples $b_{k,w}$. Figure 15 shows the 2N-DFT filter frequency response depending on the roll-off factor.

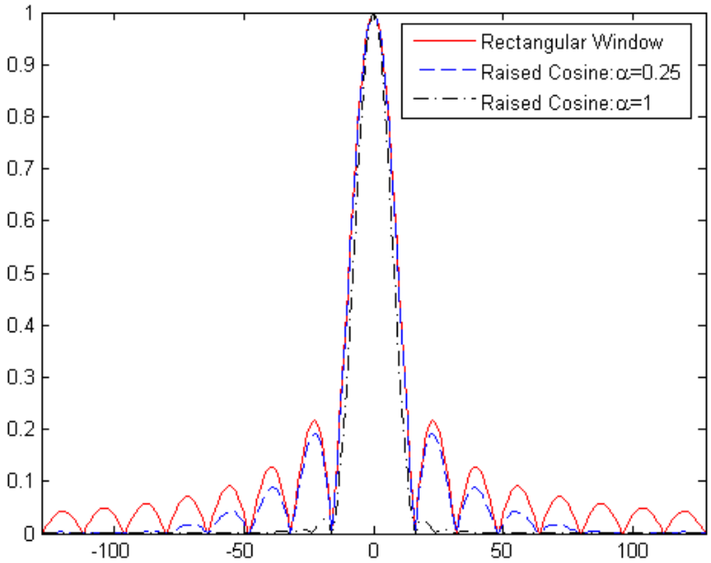


Fig. 15. Frequency response of 2N-DFT Filter with raised cosine windowing depending of roll-off factor $\alpha$

The improvement of the frequency response occurs for $\alpha > 0$. The bigger $\alpha$ turns, the lower are the frequency response side-lobes. The area covered by the filter response is smaller and the $C/N$ improves. The whole filter bank is less sensitive to frequency deviations, disturbances, etc. The reason for the improvement can also be explained through a decrease of the DFT-leakage. Since the leakage is responsible in several cases for an OFDM signal degradation, an overall improvement in demodulation is expected.

## 4. Simulation and experiment results

### 4.1 Experiment design

Figure 16 illustrates the block diagram of the underwater acoustic OFDM system[17]. The input data is first mapped into a QPSK constellation. Then the data sequence is converted in parallel and entered the FFT to perform spreading. Pilot signals are inserted before the IFFT operation which is used to implement OFDM modulation. A cyclic prefix is also appended to the data sequence as guard interval. The complex base-band digital to analog signal is then up-converted to the transmission frequency and sent out to the underwater acoustic channels by the transducer.

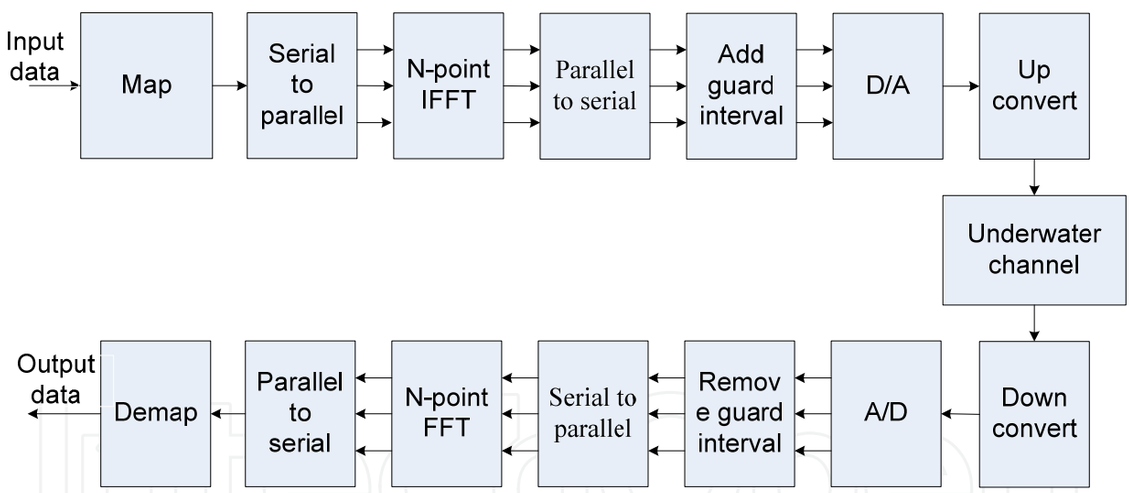


Fig. 16. Underwater acoustic OFDM system

In order to know the frame boundary, LFM signals are appended before the data sequence before transmitted into the channel. At receiver side, time synchronization is done via correlating the received samples with the known LFM sequence. After that, the received data are divided into OFDM demodulation. System specification for the experiment is shown in Table 1.

Table 2. shows the BER results of simulation with SNR=12dB for AWGN channel. The number of multipath interference is five. Each subcarrier in OFDM signal is QPSK mapped. The subcarrier number is 1024.

| | |
|---|---|
| Mapping mode | QPSK |
| Bandwidth | 6kHz |
| Carrier frequency | 30kHz |
| Transmission frequency band | 27~33kHz |
| Symbol duration | 117.3ms |

Table 1. System specification

| | **Rectangular Window** | **Raised Cosine** |
|---|---|---|
| **1** | 0.1092 | 0.0778 |
| **2** | 0.1001 | 0.0706 |
| **3** | 0.1056 | 0.0691 |
| **4** | 0.1047 | 0.0721 |
| **5** | 0.1062 | 0.0730 |
| **AVERAGE** | 0.1051 | 0.0725 |

Table 2. Simulation results

### 4.2 Experimental pool results

The experiment was carried out at the experimental pool in Xiamen University. The distance between the transmitter and the receiver is 10m.Both of them kept still during the whole experiment. The BER results of experiment were given in the Table 3, as well as the average BER. Figure 17 shows the reconstructed images using different window function in pool experiments.

| | **Rectangular Window** | **Raised Cosine** |
|---|---|---|
| **1** | 0.0799 | 0.0500 |
| **2** | 0.0791 | 0.0504 |
| **3** | 0.0773 | 0.0505 |
| **4** | 0.0781 | 0.0503 |
| **5** | 0.0785 | 0.0509 |
| **AVERAGE** | 0.0785 | 0.0504 |

Table 3. Experiment results


Fig. 17. Reconstructed images with different window function in pool experiments

### 4.3 Experimental results

The experiment was carried out in shallow water near Xiamen. Figure 18 depicts the location of transmitter and receiver transducers. The distance between transmitter and receiver was 810m. The depth of water was nearly 4m, and the transmitter and receiver were in the middle. According to the experiences before,the threshold $T$ is set 2.6. Table 4 is the result of the experiment. The BER results were given in the table, as well as the average BER. Figure 19 shows the reconstructed images using different window function in shallow water experiments.

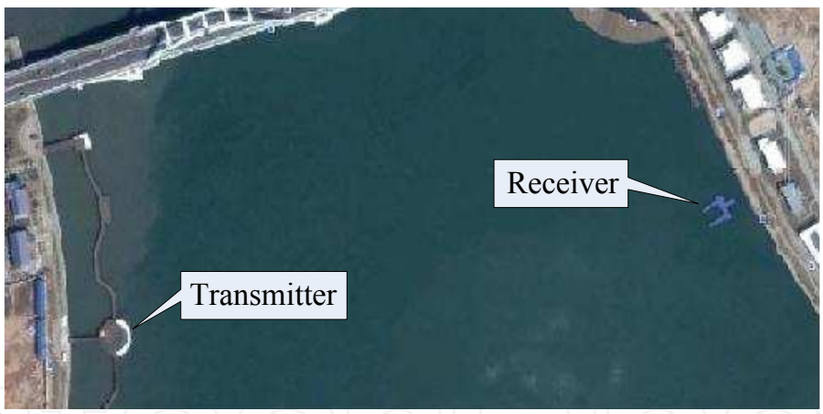


Fig. 18. The location of transmitter and receiver transducers

| | Rectangular Window | Raised Cosine |
|---|---|---|
| **1** | 0.1543 | 0.1057 |
| **2** | 0.1357 | 0.1103 |
| **3** | 0.1552 | 0.1034 |
| **4** | 0.1406 | 0.0998 |
| **5** | 0.1468 | 0.1028 |
| **AVERAGE** | 0.1465 | 0.1044 |

Table 4. Experiment results


Fig. 19. Reconstructed images with different window function in shallow water experiments

## 5. Conclusion

We propose a Raised Cosine Window for OFDM receiver and apply it to Underwater Acoustic OFDM System. Based on the results of simulation and experiment, the Raised Cosine Window applied to OFDM receiver can suppress NBI and reduce the BER, which has simple structure, and only needs a little modification in the receiver.

The proposed algorithm holds three main advantages with respect to narrowband interference suppression in underwater acoustic OFDM system. First and foremost, the simulation and the experiment results in a shallow underwater channel showed that the raised cosine window based method could achieve excellent performance. Besides, the proposed method performed comparable bandwidth efficiency to other methods. Last but not least, it need not change the frame structure of existing protocol, which is vital for the detection methods that are exploited at the receiver. The study demonstrated that the raised cosine window based narrowband interference suppression would be applicable for OFDM system over underwater acoustic channels.

## 6. References

[1] Chang, R. W., "Synthesis of Band-Limited Orthogonal Signals for Multichannel Data Transmission," Bell Systems Technical Journal, Vol. 45, December 1960, pp. 1775–1796.

[2] Saltzberg, B. R., "Performance of an Efficient Parallel Data Transmission System," IEEE Trans. on Communications, Vol. COM-15, No. 6, December 1967, pp. 805–811.

[3] Weinstein, S. B., and P. M. Ebert, "Data Transmission of Frequency Division Multiplexing Using the Discrete Frequency Transform," IEEE Trans. on Communications, Vol. COM-19, No. 5, October 1971, pp. 623–634.

[4] Peled, A., and A. Ruiz, "Frequency Domain Data Transmission Using Reduced Computational Complexity Algorithms," Proc. IEEE Int. Conf. on Acoustics, Speech, and Signal Processing (ICASSP '80), Denver, CO, 1980, pp. 964–967.

[5] S. B. Weinstein and P. M. Ebert, “Data transmission by frequency-division multiplexing using the discrete fourier transform,” IEEE Trans. Commun. , vol. 19, pp. 628–634, Oct. 1971.

[6] D. Brady and J. C. Preisig. Underwater Acoustic Communications. In H. V. Poor and G. W. Wornell, editors, Wireless Communications: Signal Processing Perspectives, chapter 8, pages 330–379. Prentice-Hall, 1998.

[7] Arthur J Redfem, “Receiver Window Design for Multicarrier Communication Systems”, IEEE Journal on Selected Areas in Communications, vol.20, no.5, Jun 2002.

[8] Hermann Rohling, “Narrow Band Interferences Reduction in OFDM based Power Line Communication Systems”, International Symposium on Power Line Communications (ISPLC) 2001.

[9] Zhang, D., Pingyi Fan, Zhigang Cao, “Receiver window design for narrowband interference suppression in IEEE 802.11a system”,Proceedings. The 2004 Joint Conference of the 10th Asia-Pacific Conference on Volume 2, 29 Aug.-1 Sept. 2004 Page(s):839-842 vol.2

[10] A. J. Redfern, “Receiver window design for multicarrier communication systems,” IEEE J. Sel. Areas Commun., vol. 20, pp. 1029–1036, 2002.

[11] Z. Wu and C. R. Nassar, “Narrowband interference rejection in OFDM via carrier interferometry spreading codes,” IEEE Trans. Wireless Commun.,vol. 4, pp. 1491–1505, 2005.

[12] D. Gerakoulis and P. Salmi, “An interference suppressing OFDM system for wireless communication,” in Proc. IEEE ICC, 2002, pp. 480–484.

[13] R. Nilsson, F. Sj¨oberg, and J. P. LeBlanc, “A rank-reduced LMMSE canceller for narrowband interference suppression in OFDM-based systems,” IEEE Trans. Commun., vol. 51, pp. 2126–2140, 2003.

[14] A. Batra and J. R. Zeidler, “Narrowband interference mitigation in OFDM systems,” in Proc. IEEE MILCOM, 2008, pp. 1–7.

[15] K. Shi, Y. Zhou, B. Kelleci, T. Fischer, E. Serpedin, and A. Karsilayan, “Impacts of narrowband interference on OFDM-UWB receivers: Analysis and mitigation,” IEEE Transactions on Signal Processing, vol. 55, no. 3, pp. 1118– 1128, Mar. 2007.

[16] K. Yip, Y. Wu, and T. Ng, “Timing-synchronization analysis for IEEE 802.11a wireless LANs in frequency-nonselective Rician fading environments,” IEEE Transactions on Wireless Communications, vol. 3, no. 2, pp. 387-394, Mar. 2004.

[17] Weijie Shen; Haixin Sun; En Cheng; Wei Su; Yonghuai Zhang; “Narrowband interference suppression in underwater acoustic OFDM system”. Informatics in Control, Automation and Robotics (CAR 2010) 2nd International Asia Conference on , Publication Year: 2010 , Page(s): 496-499.

[18] Hermann Rohling, “Narrow Band Interferences Reduction in OFDM based Power Line Communication Systems”, International Symposium on Power Line Communications (ISPLC) 2001.

[19] C. Muschallik, "EinfluR der Oszillatoren im Frontend auf ein. OFDM-Signal", Fernseh und Kinotechnik, April 1995.

[20] C. Muschallik, "Influence of RF Oscillators on an OFDM Signal", IEEE Transactions on Consumer Electronics, Vol. 41, No. 3, August 1995, pp. 592-603.
[21] C. Muschallik, V. Armbruster., “Verfahren und Schaltungsanordnung zur Verbesserung des Empfangsverhaltens bei der Ubertragung von digitalen Signalen", German Pat. appl., AZ P195 20 353.4, June 1995.

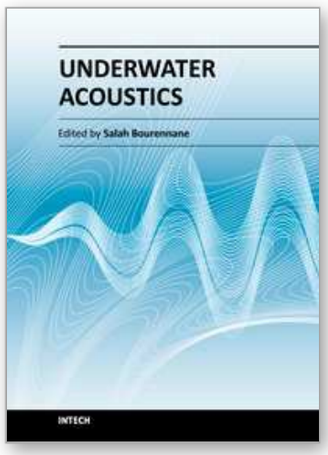


**Underwater Acoustics**
Edited by Prof. Salah Bourennane

ISBN 978-953-51-0441-4
Hard cover, 136 pages
**Publisher** InTech
**Published online** 28, March, 2012
**Published in print edition** March, 2012

**How to reference**
In order to correctly reference this scholarly work, feel free to copy and paste the following:

Weijie Shen, Haixin Sun, En Cheng, Wei Su and Yonghuai Zhang (2012). Narrowband Interference Suppression in Underwater Acoustic OFDM System, Underwater Acoustics, Prof. Salah Bourennane (Ed.), ISBN: 978-953-51-0441-4, InTech, Available from: http://www.intechopen.com/books/underwater-acoustics/narrowband-interference-suppression-in-underwater-acoustic-ofdm-system

INTECH
open science | open minds

**InTech Europe**
University Campus STeP Ri
Slavka Krautzeka 83/A
51000 Rijeka, Croatia
Phone: +385 (51) 770 447
Fax: +385 (51) 686 166
www.intechopen.com

**InTech China**
Unit 405, Office Block, Hotel Equatorial Shanghai
No.65, Yan An Road (West), Shanghai, 200040, China
中国上海市延安西路65号上海国际贵都大饭店办公楼405单元
Phone: +86-21-62489820
Fax: +86-21-62489821

IntechOpen